

Dry sliding wear behavior of extruded titanium matrix composite reinforced by in situ TiB whisker and TiC particle

Yanli Qin · Lin Geng · Dingrui Ni

Received: 4 December 2010 / Accepted: 22 February 2011 / Published online: 2 March 2011
© Springer Science+Business Media, LLC 2011

Abstract The dry sliding wear behavior of titanium matrix composite (TMC) reinforced by in situ TiB whisker and TiC particle was investigated. Compared to the unreinforced pure Ti matrix, the TMC exhibited a markedly improved wear resistance due to the existence of the ceramic reinforcements. The TMC showed lower friction coefficient than the pure Ti. The mean values of steady-state friction coefficient of the TMC and pure Ti against a tool steel were about 0.270–0.330 and 0.385–0.395, respectively, under the loads of 40–100 N. Meanwhile, the TMC showed lower weight loss and its surface wearing was less severe compared to that of the pure Ti. The worn surface of the TMC was covered with mild grooves and some fine wear debris, which exhibited the characteristic of both adhesive and abrasive. TiO_2 was found on the worn surface due to the oxidation behavior of the Ti matrix, which may reduce the wear tendency of the TMC. The results show that the in situ ceramic reinforcements could greatly increase the wear resistance of pure Ti.

Introduction

Titanium alloys are extensively used in aeronautical, marine, and chemical industries owing to their specific properties such as high strength and excellent corrosion, as well as high temperature resistance [1–3]. However, the application of titanium alloys under severe wear and friction condition is restricted due to their low hardness and poor resistance to sliding wear [4–8]. For example, the use of titanium instead of steel or cast iron in ground vehicles has the potential to reduce weight and hence increase fuel economy. However, grinding of Ti alloys is problematical because of their toughness and tendency to transfer to tooling or load the grinding wheel [8]. Surface modifications like coating and laser surface processing are attempted to improve the wear resistance of Ti alloys [9–20], but these methods are useless for improving the strength and hardness of the alloys.

Composite materials offer many advantages over traditional metallic materials. With incorporation of ceramic particles into titanium alloys, titanium matrix composites (TMCs) are provided with better hardness, strength, and wear resistance [21–23]. Furthermore, TMCs reinforced by in situ ceramic particles received extensive research interest due to the low cost, ease fabrication, and excellent interface bonding strength [22, 23], especially those reinforced by in situ titanium boride (TiB) or/and titanium carbide (TiC) [24–31].

TiB and TiC can provide a strong reinforcement-matrix bonding strength due to the good thermodynamic stability with titanium [22, 23]. This may reduce the pull-out of the reinforcement from the matrix during sliding. So the in situ TiB or/and TiC are expected to provide TMCs with good wear resistance [7, 8, 32–34]. However, information is not enough on the tribological and wearing behavior of the in

Y. Qin (✉)
School of Science, Shenyang Ligong University,
Shenyang 110168, China
e-mail: qyl0628@yahoo.com.cn

L. Geng
School of Materials Science and Engineering, Harbin Institute of Technology, P.O. Box 433, Harbin 150001, China

D. Ni
Shenyang National Laboratory for Materials Science,
Institute of Metal Research, Chinese Academy of Sciences,
72 Wenhua Road, Shenyang 110016, China

situ TiB and TiC reinforced TMCs, especially few investigations are reported on the as-extruded TMCs. In the present study, we studied the sliding wear behavior of an as-extruded TMC reinforced by in situ TiB whisker (TiBw) and TiC particle (TiCp), with the aim to understand the effect of the reinforcements on the wear behavior of the composite.

Materials and methods

10 vol.% (TiBw + TiCp)/Ti composite was prepared based on the reaction of $5\text{Ti} + \text{B}_4\text{C} = 4\text{TiB} + \text{TiC}$. Commercial titanium (Ti) powders (99% purity) and boron carbide (B_4C) powders (99% purity) with an average size of 10 and 0.5 μm , respectively, were used as raw materials. The blended powders were firstly hot pressed in vacuum and then extruded into rods of 12 mm diameter at an extrusion ratio of 16:1. The unreinforced pure Ti was produced in a similar manner for comparison. Phase identification of the as-extruded composites was conducted via XRD using a Phillipx'pert X-ray diffractometer and Cu K α radiation, with the sample surfaces paralleling to the extrusion direction. Vickers hardness tests (HV-5) were conducted on the transverse section of the extruded samples by using a HV-200 tester under the condition of 5 kg load for 20 s. For scanning electron microscopic (SEM, HITACHI S-4700) analysis, the TMC samples parallel and perpendicular to the extrusion direction were polished and etched ($\text{H}_2\text{O}:\text{HNO}_3:\text{HF} = 85:10:5$). Transmission electron microscopic (TEM) studies were performed using a Philips CM-12 microscope operated at 120 kV. Thin foil samples sectioned perpendicular to the extrusion direction were prepared using standard techniques involving mechanical grinding and ion milling.

Cylindrical samples with a diameter of 5 mm and a length of 20 mm were machined by electro-discharge machining from the extruded bars, with the axis paralleling to the extrusion direction. Sliding wear tests were carried out on a pin-on-disk machine under the normal loads ranging from 40 to 100 N, with a sliding velocity of about 0.54 m/s. All tests were performed at room temperature in air without any lubricants. The total sliding distance was about 212 m for each wear test. A circular disk with a diameter of 34 mm and a thickness of 10 mm was used as the counter disk, which was made of a tool steel with the surface hardness of >58 HRc and surface roughness of $\text{Ra} = 1 \mu\text{m}$. Wear was determined by measuring the mass loss of samples using a precision balance (0.1 mg). The worn surface and the debris of samples were examined using SEM. The wear surfaces were analyzed using a PHI 5700 X-ray photoelectron spectrometer (XPS).

Results and discussion

Microstructures

The XRD results of the as-sintered materials showed that the B_4C powders disappeared and TiB and TiC were formed after the sintering (Fig. 1). The SEM microstructures of the composite showed that rod-like TiBw with a diameter of less than 0.3 μm and an aspect ratio of about 20 were aligned along the extrusion direction in the TMC (Fig. 2a, b). Almost no TiCp were visible in the SEM microstructures, and this is attributed to their fine size. Furthermore, the TEM examinations showed that the TiBw exhibited a hexagonal cross-section, and the TiCp was in an equiaxed morphology (Fig. 2c). The Vickers hardness of the pure Ti and TMCs was about 315 and 580 (HV-5), respectively, and the latter was much higher than the former with an increase of about 84%.

Friction coefficient

Figure 3 shows the friction coefficient of the pure Ti and TMC samples under the load of 40–100 N, respectively. Three important observations can be made. First, the friction coefficients all increased at the start of sliding ($\sim 20 \text{ m}$) and then reached a steady state. Second, the mean values of steady-state friction coefficient of the pure Ti and TMC are about 0.385–0.395 and 0.270–0.330, respectively, and the TMC showed a much lower friction coefficient than the pure Ti. Third, the friction coefficient of the pure Ti was relatively stable under the applied loads whereas that of the TMC decreased with increasing the load.

The pure Ti showed higher friction coefficient and this is due to its ductile nature and low work hardening ability [18]. Compared to the pure Ti, the TMCs showed much lower friction coefficient and this should be attributed to the formation of TiBw and TiCp reinforcements which produce a higher hardness and strength of the materials. This will be discussed in “Worn surface” section.

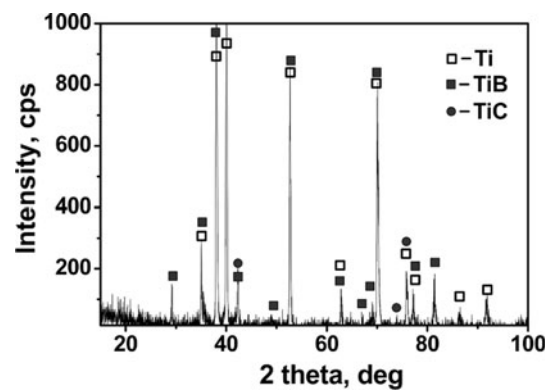


Fig. 1 XRD results of as-extruded TMC

Fig. 2 SEM micrographs of as-extruded TMC parallel (**a**) and perpendicular (**b**) to extrusion direction, and (**c**) TEM showing fine TiCp

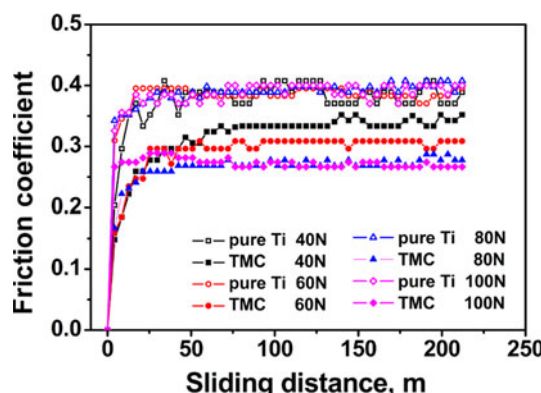
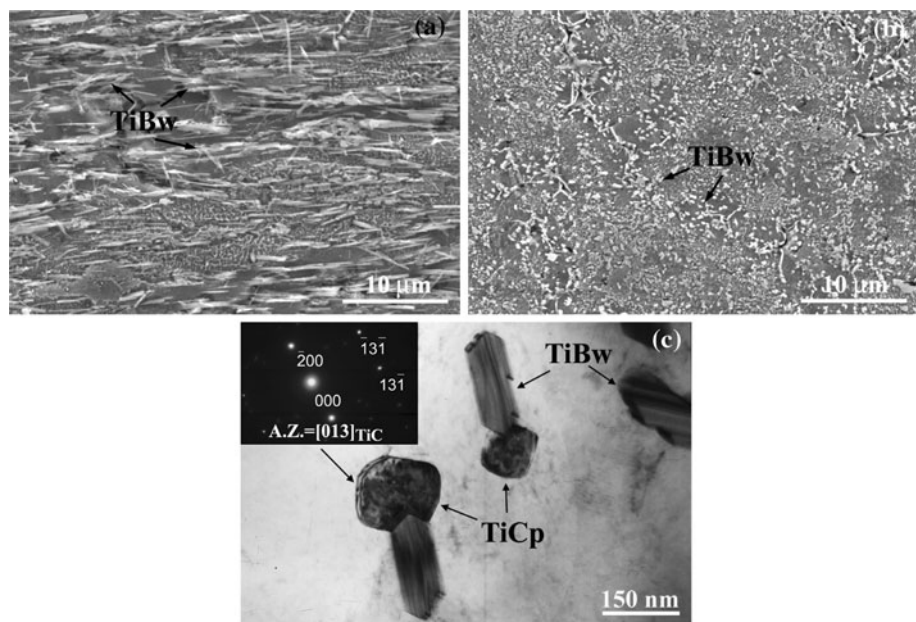


Fig. 3 Friction coefficients of Pure Ti and TMC samples as a function of sliding distance

Weight loss

Figure 4 shows the weight loss of samples under loads of 40 to 100 N, with a sliding distance of 212 m. Under the load of 40, 60, 80, and 100 N, the weight loss of the TMC was 18.7, 18.8, 13.4, and 10.4% of that of the pure Ti, respectively. As can be seen, the TMC samples showed remarkably lower weight loss compared to the pure Ti samples. Moreover, the TMC exhibited better advantage under higher loads. The improvement of the wear resistance is attributed to the evenly distributed TiBw and TiCp, and this will be discussed later.

Worn surface

Figure 5 shows the worn surface of the pure Ti and TMC samples tested under an applied load of 100 N. In the case

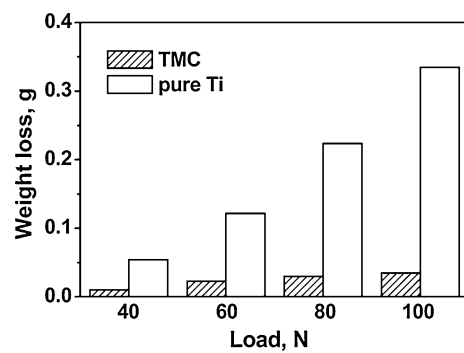


Fig. 4 Weight loss of pure Ti and TMC samples with a sliding distance of 212 m

of the pure Ti, the heavy deformation and tearing were apparent and the worn surface was covered by severe flakes and long grooves which showed the typical characteristics of severe adhesive. This surface morphology formed as the counter body ploughed across the surface and eventually removed material from the worn surface primarily through ductile processes. Compared to that of the pure Ti, the surface wearing of the TMC was less severe and there were mild grooves with some fine wear debris on the worn surface. This kind of morphology exhibited the characteristic of both adhesive and abrasive. As the soft Ti matrix was removed from the surface, the hard ceramic reinforcements were exposed and worn against the counter body, which effectively protected the matrix during sliding.

Figure 6 shows the etched cross-section of worn surfaces of the pure Ti and TMC samples. For the pure Ti sample, the worn surface was rough. There was a plastic deformed subsurface about 35 μm in thickness under the worn surface. Many pores were apparently visible in the

Fig. 5 SEM micrographs of worn surfaces of pure Ti (a) and TMC (b) samples under load of 100 N

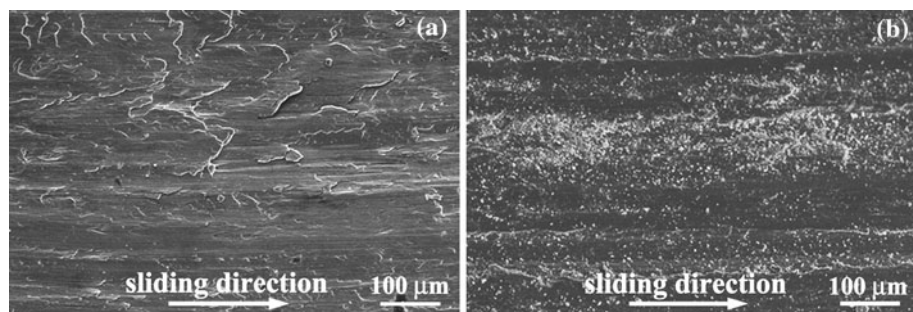
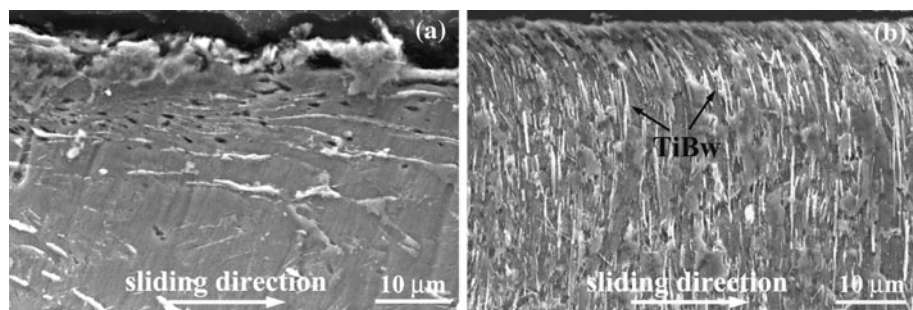


Fig. 6 Etched cross-section of worn surfaces of pure Ti (a) and TMC (b) samples under load of 100 N



subsurface. Those pores should be resulted from the defects such as micro-cracks which were generated by the plastic deformation during the process of friction and wear. The results revealed that the plastic deformed region was likely to be formed in the subsurface of the Ti matrix during the process of friction and wear due to the low strength and stiffness. Compared to the pure Ti sample, the TMC sample showed a relatively smooth worn surface. A much shallower plastic deformation subsurface about 15 μm in thickness was found under the worn surface, but no visible pores appeared in this region. Meanwhile, many TiBw in the subsurface were found to be broken and bent toward the sliding direction. As can be seen, no separation of TiBw from the matrix was observed and this shows that strong interface bonding strength occurred between the reinforcements and matrix.

It is apparent from the worn surfaces that the TMC exhibited better wear resistance, and this should be ascribed to the following reasons. First, the TiBw and TiCp greatly increased the strength and hardness of the TMC so it could retard the defects from being formed in the subsurface. Second, the TiBw and TiCp are hard and stiff with good wear resistance. After the soft titanium matrix was recessed, they would wear against the disk material, thereby retarding further wear of the matrix. Third, the strong interfacial bonding strength can effectively prevent the reinforcements from being pullout and pin up the Ti matrix during wear, so it is difficult for the wear debris to flake off under shear stress. Fourth, as discussed above, the TMC showed lower friction coefficient and this can be

easily concluded from the quite different morphologies of the worn surfaces between the pure Ti and TMC samples. This lower friction coefficient may greatly decrease the wear tendency.

Wear debris

The wear debris of the pure Ti and TMC exhibited similarly lamellar morphology (Fig. 7). However, the former showed large sizes with the width of more than 200 μm, and the latter showed much smaller sizes of less than 100 μm. The difference should be also attributed to the presence of the TiBw and TiCp which prevented the cracks from being formed and extended within the matrix. Thus, the formation of a spall on the wear track was retarded by the reinforcements and it was difficult for the large lamellar spall to form on the worn surface.

Another issue that should be taken into consideration is the oxidation behavior of the TiBw and the Ti matrix. During the sliding process, the heat resulting from the friction increased the temperature, which could result in the oxidation of the TiBw on the worn surfaces. It was reported [35] that TiB would be oxidized into titanium dioxide (TiO_2) and boron oxide (B_2O_3) at high temperatures according to the following reaction: $2TiB(s) + 7/2O_2(g) \rightarrow 2TiO_2(s) + B_2O_3$ (solid if $T < 723$ K, and liquid if $T > 723$ K). Subsequently B_2O_3 would react with the water from the environment to form boric acid (H_3BO_3) ($1/2B_2O_3 + 3/2H_2O \rightarrow H_3BO_3$). Both B_2O_3 and H_3BO_3 could act as solid lubricants so as to alleviate the friction

Fig. 7 SEM micrographs of debris of pure Ti (a) and TMC (b) samples under load of 100 N

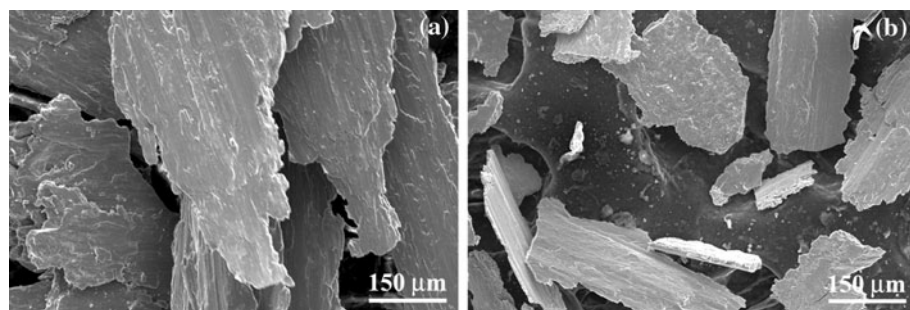
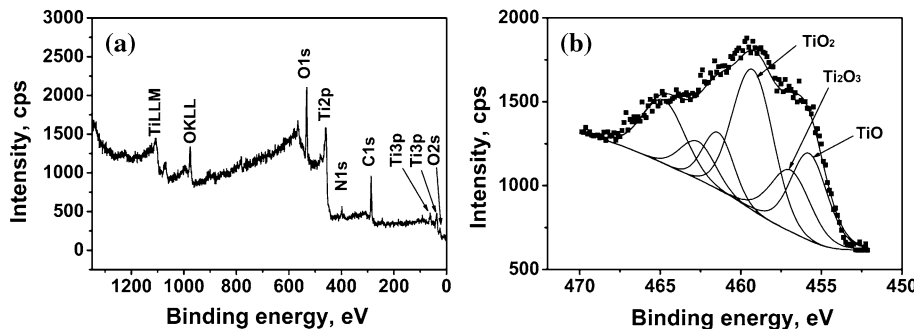


Fig. 8 XPS survey scans (a) and Ti spectra (b) of worn surface of TMC under load of 100 N



and wear of the TMCs [36, 37], and this would be partially responsible for the better wear resistance of the TMC.

The XPS spectrum of the worn surface of the TMC sample (Fig. 8) shows that the elements were mainly Ti and O (Fig. 8a). The peak of C1s (286.8 eV) and N1s (398.0 eV) came from the C and N of the ambient air. The Ti spectrum further indicates that the surface mainly contained TiO₂ and a small amount of Ti₂O₃ and TiO, which were resulted from the oxidation of Ti element during the test (Fig. 8b). It was pointed out that the oxide surface layer formed on titanium alloys was ready to transfer and adhere to both metallic and nonmetallic surfaces, resulting in severe adhesive wear [7], whereas some extremely fine TiO₂ particles on the TMC could be an excellent solid lubricant which could release the friction and wear of TMC and increase its wear resistance [38, 39]. However, the element of B and C could not be detected from the XPS spectrum due to their quite low contents. Consequently, it was also difficult to determine the formation of B₂O₃ and H₃BO₃.

Conclusions

- (1) TiBw and TiCp hybrid-reinforced TMCs were fabricated by reactive hot pressing. The in situ formed ceramic reinforcements significantly improved the wear resistance of the TMC.
- (2) The TMC showed an apparently lower friction coefficient than the pure Ti. Under the loads of 40–100 N, the mean values of steady-state friction coefficient of

the TMC and pure Ti against the tool steel were about 0.270–0.330 and 0.385–0.395, respectively.

- (3) The worn surface of the pure Ti was characterized by severe flakes and long grooves which showed a typical adhesive wear mode, whereas that of the TMC was less severe and there were mild grooves with some fine wear debris on the worn surface, which exhibited the characteristic of both adhesive and abrasive.
- (4) TiBw and TiCp greatly reduced the plastic deformation subsurface of the unreinforced pure Ti. TiBw were broken and bent toward the sliding direction in the subsurface but no separation of TiBw from the matrix was observed.
- (5) The debris of the pure Ti and TMC samples showed a similar lamellar morphology. The former showed large sizes with the width of more than 200 μm, and the latter showed much smaller sizes of less than 100 μm.
- (6) TiO₂ was formed on the worn surface due to the oxidation behavior of the Ti matrix, but it was difficult to determine the formation of B₂O₃ and H₃BO₃ due to the low content of B element.

Acknowledgement This study is financially supported by National Natural Science Foundation of China under grant no. 50771039.

References

1. Brewer WD, Bird RK, Wallace TA (1998) Mater Sci Eng A 243:299
2. Seagle SR (1996) Mater Sci Eng A 213:1

3. Yamada M (1996) *Mater Sci Eng A* 213:8
4. Marc L, Rack HJ (2001) *Wear* 249:158
5. La PQ, Ma JQ, Zhu YT, Yang J, Liu WM, Xue QJ, Valiev RZ (2005) *Acta Mater* 53:5167
6. Lakshmi SG, Arivuoli D (2006) *Tribol Int* 39:548
7. Alman DE, Hawk JA (1999) *Wear* 225–229:629
8. Blau PJ, Jolly BC (2009) *JMEPEG* 18:424
9. Wang F, Bi QL, Wang XB, Liu WM (2008) *Tribol Int* 41:158
10. Ocelík V, Matthews D, De Hosson JThM (2005) *Surf Coat Technol* 197:303
11. Atar E, Kayali ES, Cimenoglu H (2008) *Surf Coat Technol* 202:4583
12. Lee CS, Oh JC, Lee S (2003) *Metall Mater Trans A* 34:1461
13. Pu YP, Guo BG, Zhou JS, Zhang ST, Zhou HD, Chen JM (2008) *Appl Surf Sci* 255:2697
14. Dong YJ, Wang HM (2009) *Surf Coat Technol* 204:731
15. Candel JJ, Amigó V, Ramos JA, Busquets D (2010) *Surf Coat Technol* 204:3161
16. Zhang S, Wu WT, Wang MC, Man HC (2001) *Surf Coat Technol* 138:95
17. Zhou W, Zhao YG, Li W, Mei XL, Jiang QC (2008) *Surf Coat Technol* 202:1652
18. Lee C, Sanders A, Tikekar N, Chandran KSR (2008) *Wear* 265:375
19. Wang F, Mei J, Jiang H, Wu X (2007) *Mater Sci Eng A* 445–446:461
20. Hu RH, Lim JK (2010) *Mater Des* 31:2670
21. Ranganath S (1997) *J Mater Sci* 32:1
22. Tjong SC, Ma ZY (2000) *Mater Sci Eng R* 29:49
23. Tjong SC, Mai YW (2008) *Compos Sci Technol* 68:583
24. Ma ZY, Tjong SC, Geng L (2000) *Scripta Mater* 42:367
25. Lu WJ, Zhang D, Zhang XN, Wu RJ, Sakata T, Mori H (2001) *Scripta Mater* 44:2449
26. Gorsse S, Miracle DB (2003) *Acta Mater* 51:2427
27. Chandran KSR, Panda KB, Sahay SS (2004) *JOM* 56:42
28. Saito T (2004) *JOM* 56:33
29. Panda KB, Chandran KSR (2006) *Acta Mater* 54:1641
30. Morsi K, Patel VV (2007) *J Mater Sci* 42:2037. doi: [10.1007/s10853-006-0776-2](https://doi.org/10.1007/s10853-006-0776-2)
31. Ni DR, Geng L, Zhang J, Zheng ZZ (2008) *Mater Lett* 62:686
32. Hibi Y, Murakami T, Miyake K, Sasaki S (2008) *J Am Ceram Soc* 91:508
33. Miyoshi K, Sanders JH, Hager CH Jr, Zabinski JS, Vander Wal RL, Andrews R, Street KW Jr, Lerch BA, Abel PB (2008) *Tribol Int* 41:24
34. Dalili N, Edrisy A, Farokhzadeh K, Li J, Lo J, Riahi AR (2010) *Wear* 269:590
35. Zhang EL, Zeng G, Zeng SY (2002) *Scripta Mater* 46:811
36. Caracostas CA, Chiou WA, Fine ME, Cheng HS (1997) *Metall Mater Trans A* 28:491
37. Zhao M, Wu GH, Jiang LT, Dou ZY (2006) *Composites A* 37:1916
38. Li JL, Sun MR, Ma XX, Tang GZ (2006) *Wear* 261:1247
39. Song HJ, Zhang ZZ (2008) *Tribol Int* 41:396